J|A|C|S
ARTICLES
Published on Web 08/09/2006

Cyclization and Catenation Directed by Molecular Self-Assembly

Wei Wang,[†] LiQiong Wang,[‡] Bruce J. Palmer,[‡] Gregory J. Exarhos,[‡] and Alexander D. Q. Li*,[†]

Contribution from the Department of Chemistry, Washington State University, Pullman, Washington 99164, and Chemical Sciences Division, Pacific Northwest National Laboratory, Richland, Washington 99352

Received March 16, 2006; E-mail: dequan@wsu.edu

Abstract: We report here that molecular self-assembly can effectively direct and enhance specific reaction pathways. Using perylene $\pi-\pi$ stacking weak attractive forces, we succeeded in synthesizing perylene bisimide macrocyclic dimer and a concatenated dimer−dimer ring from dynamic self-assembly of monomeric bis-*N*,*N*′-(2-(2-(2-(2-thioacetylethoxy)ethoxy)ethoxy)ethyl)perylenetetracarboxylic diimide. The monocyclic ring closure and the dimer−dimer ring concatenation were accomplished through formation of disulfide bonds, which was readily triggered by air oxidization under basic deacetylation conditions. The perylene cyclic dimer and its concatenated tetramer were characterized using both structural methods (NMR, mass spectroscopy) and photophysical measurements (UV−vis spectroscopy). Kinetic analyses offer informative insights about reaction pathways and possible mechanisms, which lead to the formation of complex concatenated rings. Molecular dynamic behaviors of both the monocyclic dimer and the concatenated dimer−dimer ring were modeled with the NWChem molecular dynamics software module, which shows distinct stacking activities for the monocyclic dimer and the concatenated tetramer.

Introduction

Molecular interactions driven by aromatic $\pi-\pi$ stacking via molecular orbital overlap have the capacity to direct supramolecular assembly or macromolecular folding in a controlled manner.[1] Strategies using electron-rich π-donor and electron-poor π-acceptor pairs,[2] metal-chelated $\pi-\pi$ conjugation (e.g., nanomachinery created by Stoddart and co-workers),[3] and hydrophobic $\pi-\pi$ aggregation via amphiphilic solvation[4] have been successfully demonstrated to form cyclic and/or concatenated rings. Many ring closures use disulfide bonds, which can form and break reversibly; the desired product is often amplified from dynamic combinatorial libraries using weak host−guest interactions to template the formation of the product at the expense of unfit library members.[5] It is well-known that perylene bisimide dyes form π-stacked structures in crystals.[6] However, π-stacking, thus far, is usually considered as a secondary motif, with other noncovalent interactions such as hydrogen bonding as the major driving force for promoting self-organization in solution.[7]

Current studies on molecular self-assembly mostly finish by characterizing the structural features of the self-organized nano-objects, such as nanospheres or nanorods. We would like to emphasize that molecular self-assemblies have the capacity to direct specific reaction pathways that are otherwise difficult to achieve. Specifically, we use $\pi-\pi$ interactions as the major driving force to influence the reaction pathways of cyclization and concatenation of perylene derivatives. No template is needed as the reactants undergo the assembly process by self-templating.

[†] Washington State University.
[‡] Pacific Northwest National Laboratory.

(1) (a) Hoeben, F. J. M.; Jonkheijm, P.; Meijer, E. W.; Schenning, A. P. H. J. *Chem. Rev.* **2005**, *105*, 1491−1546 and references therein. (b) Franceschin, M.; Alvino, A.; Ortaggi, G.; Bianco, A. *Tetrahedron Lett.* **2004**, *45*, 9015−9020. (c) Rowan, S. J.; Cantrill, S. J.; Cousins, G. R. L.; Sanders, J. K. M.; Stoddart, J. F. *Angew. Chem., Int. Ed.* **2002**, *41*, 898−952.
(2) (a) Gabriel, G. J.; Sorey, S.; Iverson, B. L. *J. Am Chem. Soc.* **2005**, *127*, 2637−2640. (b) Neuteboom, E. E.; Van Hal, P. A.; Janssen, R. A. *Chem.−Eur. J.* **2004**, *10*, 3907−3918 and references therein. (c) Kieran, A. L.; Pascu, S. I.; Jarrosson, T.; Gunter, M. J.; Sanders, J. K. M. *Chem. Commun.* **2005**, 1842−1844.
(3) (a) Stoddart, J. F.; Tseng, H.-R. *Proc. Natl. Acad. Sci. U.S.A.* **2002**, *99*, 4797−4800. (b) Raehm, L.; Kern, J.-M.; Sauvage, J.-P.; Hamann, C.; Palacin, S.; Bourgoin, J.-P. *Chem.−Eur. J.* **2002**, *8*, 2153−2162. (c) Kaiser, G.; Jarrosson, T.; Otto, S.; Ng, Y.-F.; Bond, A. D.; Sanders, J. K. M. *Angew. Chem., Int. Ed.* **2004**, *43*, 1959−1962. (d) Aricó, F.; Badjic, J. D.; Cantrill, S. J.; Flood, A. H.; Leung, K. C.-F.; Liu, Y.; Stoddart, J. F. *Top. Curr. Chem.* **2005**, 203−259. (e) Fuller, A. M. L.; Leigh, D. A.; Lusby, P. J.; Slawin, A. M. Z.; Walker, D. B. *J. Am. Chem. Soc.* **2005**, *127*, 12612−12619. (f) Leigh, D. A.; Lusby, P. J.; Slawin, A. M. Z.; Walker, D. B. *Angew. Chem., Int. Ed.* **2005**, *44*, 4557−4564.
(4) Rossetti, L.; Franceschin, M.; Bianco, A.; Ortaggi, G.; Savino, M. *Bioorg. Med. Chem. Lett.* **2002**, *12*, 2527−2533.
(5) (*a*) Otto, S.; Furlan, R. L. E.; Sanders, J. K. M. *Science* 2002, *297*, 590−593. (b) Krishnan-Ghosh, Y.; Balasubramanian, S. *Angew. Chem., Int. Ed.* **2003**, *42*, 2171−2173. (c) Leclaire, J.; Vial, L.; Otto, S.; Sanders, J. K. M. *Chem. Commun.* **2005**, *15*, 1959−1961. (d) Hioki, H.; Still, W. C. *J. Org. Chem.* **1998**, *63*, 904−905. (e) Otto, S.; Furlan, R. L. E.; Sanders, J. K. M. *J. Am. Chem. Soc.* **2000**, *122*, 12063−12064. (f) Corbett, P. T.; Sanders, J. K. M.; Otto, S. *J. Am. Chem. Soc.* **2005**, *127*, 9390−9392. (g) Corbett, P. T.; Tong, L. H.; Sanders, J. K. M.; Otto, S. *J. Am. Chem. Soc.* **2005**, *127*, 8902−8903.
(6) Würthner, F. *Chem. Commun.* **2004**, 1564−1579.
(7) (a) Hansen, J. G.; Feeder, N.; Hamilton, D. G.; Gunter, M. J.; Becher, J.; Sanders, J. K. M. *Org. Lett.* **2000**, *2*, 449−452. (b) Würthner, F.; Thalacker, C.; Sautter, A. *Adv. Mater.* **1999**, *11*, 754−758. (c) Würthner, F.; Thalacker, C.; Sautter, A.; Schärtl, W.; Ibach, W.; Hollricher, O. *Chem.−Eur. J.* **2000**, *6*, 3871−3886. (d) Würthner, F.; Hanke, B.; Lysetska, M.; Lambright, G.; Harms, G. S. *Org. Lett.* **2005**, *7*, 967−970. (e) Hou, J.-L.; Shao, X.-B.; Chen, G.-J.; Zhou, Y.-X.; Jiang, X.-K.; Li, Z.-T. *J. Am. Chem. Soc.* **2004**, *126*, 12386−12394. (f) Faul, C. F. J.; Antonietti, M. *Chem.−Eur. J.* **2002**, *8*, 2764−2768.

10.1021/ja061826p CCC: $33.50

In these reactions, molecular self-assembly serves as the precursor for cyclization and concatenation reactions. Such a molecular assembly has an optimal configuration similar to the transition-state activation complex, which promotes certain reaction pathways and discourages others. In essence, molecular self-assembly, which serves to preorganize reactants, effectively lowers the entropic barrier from normally chaotic reactants into an organized transition state.

Considering that such π-stacking could take place in organic solvents,[8] we report that the dynamic self-assembly (DSA) of bis-*N*,*N*′-(2-(2-(2-(2-thioacetylethoxy)ethoxy)ethoxy)ethyl)-perylenetetracarboxylic diimide (**1**), directed by $\pi-\pi$ attraction, leads to the syntheses of a cyclic perylene dimer (**2**) and a dimer−dimer catenane (**4**) via disulfide linkages.

Experimental Section

1. Characterization Techniques: MALDI mass spectra were obtained with an ABVS-2025 spectrometer. ^{1}H NMR spectra were recorded with a Mercury 300 (300 MHz) or an Inova 500 (500 MHz) spectrometer at ambient temperature. ^{13}C NMR spectra were recorded at 75.48 MHz with a Mercury 300 spectrometer or at 125.7 MHz with an Inova 500 (500 MHz) spectrometer. The solvent for solution NMR is $CDCl_3$ or CD_3OD, and the central line of $CDCl_3$ at 77.00 ppm was used as a reference for ^{13}C spectra. Reaction progress was monitored by HPLC (Agilent 1100 Series) using CH_2Cl_2/MeOH as an eluant and thin-layer chromatography (TLC) on a precoated plate of silica gel 60 F_{254} (EM Science). TLC detection was made visible by charring the TLC plates with sulfuric acid. Column chromatography, unless stated otherwise, was performed on silica gel 60 (230−400 mesh, EM Science).

2. Synthesis: Preparation of bis-*N*,*N*′-(2-(2-(2-(2-thioacetylethoxy)-ethoxy)ethoxy)ethyl)perylenetetracarboxylic diimide (**1**) was achieved according to the procedures described in the Supporting Information.

3. General Procedure for Preparation of Monocyclic Dimer 2 and its Catenane 4. To a series of CH_2Cl_2 solutions of acetyl dithiols (**1**) in open flasks at concentrations of 2.58 mM, 0.58 mM, and 0.1 mM, respectively, were added several drops of 2 M NaOMe/MeOH; this made the reaction mixtures change color from red to dark blue at pH 8 to 9. The resulting dithiol derivative, formed from deacetylation of **1**, was an unstable intermediate and started to form disulfide bonds where the geometric requirements were favorable under air and the disulfide bonds were able to interchange in situ until favorable products were formed.[9,10] HPLC monitoring of the equilibrium system indicated two major products at the end of the reaction. For example, at the concentration of 0.58 mM, results from the HPLC measurement indicated that the isolated yields of the two major products were ∼39% for the dimer-based monocyclic disulfide **2** and ∼36% for its catenane **4** after neutralization of the reactions (Supporting Information). The thin-layer chromatography (TLC) detection also showed that the reaction had produced the cyclic oligomers (R_f 0.24 to 0.42, CH_2Cl_2/MeOH: 20/1). There were unidentified chromophores polymerized in situ on the TLC plate with R_f 0.0 regardless of the nature of the elution solvent used. TLC detection of the disulfide dynamic self-assembling systems at different concentrations demonstrated that the **2** and **4** structures were the major products at the end.

3.1. Method 1. Concentration (2.6 mM) of 1 above Critical Concentration of Self-Organization. To a solution of **1** (111 mg, 0.129 mmol) in CH_2Cl_2 (50 mL) was added NaOMe (0.25 mL, 2 M in MeOH) dropwise, and the color of the reaction mixture changed from red to purple to dark blue. After 15−20 min at rt, methanol (10 mL) was added to the reaction mixture, and two main products emerged within 5 min, as seen by TLC monitoring. The reaction was then neutralized with Amberlite IR-120 (H^+) resin, filtered, concentrated, and flash chromatographed (SiO_2, 10/1, CH_2Cl_2/MeOH) to give the monocyclic dimer ring **2** and the concatenated rings **4**. Further purification of compound **4** was carried out using HPLC (column: Zorbax RX-Sil, 5 μm; solvent: 100/4.5, CH_2Cl_2/MeOH). For compound **2**: R_f 0.41, CH_2Cl_2/MeOH (20/1).^{1}H NMR ($CDCl_3$, 300 MHz) δ 8.28 (d, J = 8.1 Hz, 8 H, Hα: outside protons on perylene ring), 7.98 (d, J = 8.1 Hz, 8 H, Hβ: inside protons on the perylene ring), 4.47 (bt, J = 6.0 Hz, 8 H, Hχ: on tetraethylene glycol), 3.96 (bt, J = 6.0 Hz, 8 H, Hδ: on tetraethylene glycol), 3.84−3.78 (m, 8 H, Hϵ: on tetraethylene glycol), 3.76−3.70 (m, 8 H, Hϕ: on tetraethylene glycol), 3.68−3.60 (m, 16 H, Hγ, Hι: on tetraethylene glycol), 3.60−3.54 (m, 8 H, Hη: on tetraethylene glycol), 2.74 (t, J = 6.4 Hz, 8 H, Hφ: on tetraethylene glycol). ^{1}H NMR assignments were based on ^{1}H−^{1}H COSY and GOESY (NOE)] ^{13}C NMR ($CDCl_3$, 125.7 MHz) δ 162.8 (C-carbonyl), 133.5 (Cκ), 130.7 (Ca), 128.6 (Cμ), 125.3 (Cν or Cλ), 122.8 (Cλ or Cν), 122.5 (Cβ), 70.8 (Cϕ), 70.6 (Cγ), 70.4 (Cη), 70.3 (Cϵ), 69.4 (Cι), 67.9 (Cδ), 39.5 (Cχ), 38.6 (Cφ). The ^{13}C NMR chemical shifts were assigned based on ^{1}H−^{13}C COSY (HMQC) and CIGAR experiments (see Supporting Information Figure 1 for details of the assignments). MS (MALDI): *m*/*z* 1545.8 $[M + H]^+$, 1567.8 $[M + Na]^+$, 1581.8 $[M + H + 2H_2O]^+$. For compound **4**: R_f 0.31, CH_2Cl_2/MeOH (20/1). ^{1}H NMR ($CDCl_3$/CD_3OD, 20/1, 500 MHz) δ 7.78 (d, J = 8.0 Hz, 16 H, Hα: outside protons on the perylene ring), 7.34 (d, J = 8.0 Hz, 16 H, Hβ: inside protons on the perylene ring), 4.29 (bt, J = 5.5 Hz, 16 H, Hχ: on tetraethylene glycol), 3.84 (bt, J = 5.5 Hz, 16 H, Hδ: on tetraethylene glycol), 3.79−3.75 (m, 16 H, Hϵ: on tetraethylene glycol), 3.75−3.70 (m, 32 H, Hϕ, Hι: on tetraethylene glycol), 3.70−3.66 (m, 16 H, Hγ: on tetraethylene glycol), 3.65−3.60 (m, 16 H, Hη: on tetraethylene glycol), 2.90 (t, J = 6.5 Hz, 16 H, Hφ: on tetraethylene glycol). The ^{1}H NMR assigments (see Supporting Information Figure 1) were based on ^{1}H−^{1}H COSY and GOESY (NOE). ^{13}C NMR ($CDCl_3$/CD_3OD, 20/1, 75.48 MHz) δ 162.4, 132.7, 130.1, 127.7, 124.3, 122.2, 70.8, 70.6, 70.4, 70.2, 69.6, 68.0, 39.5, 38.7. MS (MALDI): *m*/*z* 3090.2 $[M + H]^+$, 3106.7 $[M + H + H_2O]^+$, 3111.5 $[M + Na]^+$, 3125.3 $[M + H + 2H_2O]^+$, 1544.7 $[M/2]^+$, 1566.7 $[M/2 + Na]^+$, 1580.6 $[M/2 + 2H_2O]^+$.

3.2. Method 2. Concentration (0.58 mM or 0.1 mM) of 1 at or Near Critical Concentration of Self-Organization. To a solution of **1** (100 mg, 0.117 mmol) in CH_2Cl_2 (200 mL) or (50 mg, 0.058 mmol) in CH_2Cl_2 (500 mL) was added 2 M NaOMe in MeOH (5 drops/100 mL) dropwise, and the color of the reaction mixture changed from red to purple and then to blue. After 10−40 min at rt, two main products appeared. The reaction was subsequently neutralized with Amberlite IR-120 (H^+) resin, and the products were filtered, concentrated, and purified with flash chromatography (SiO_2, 10/1, CH_2Cl_2/MeOH) to give the monocyclic dimer ring **2** and its concatenated ring structure of **4**. For the lower concentration, 0.03 mM, monocyclic perylene monomer **3** (see supporting Figure 3) could be obtained as the third final product following the exact procedure described for the higher concentrations of 0.58 mM or 0.1 mM of **1**.

Results and Discussion

1. Self-Assembly Directed Synthesis. To illustrate the relationship between DSA and reaction products, we employ **1** or AcS-perylene-SAc,[10] which undergoes appreciable self-organization, forming a twisted π-cofacial conformation above its critical concentration region, C_c ∼0.1−1.0 mM in $CHCl_3$

(8) (a) Bert, V.; Huc, I.; Khoury, R. G.; Krische, M. J.; Lehn, J.-M. *Nature* **2000**, *407*, 720−723. (b) Zubarev, E. R.; Pralle, M. U.; Sone, E. D.; Stupp, S. I. *J. Am. Chem. Soc*. **2001**, *123*, 4105−4106. (c) Orr, G. W.; Barbour, L. J.; Atwood, J. L. *Science* **1999**, *285*, 1049−1052.
(9) Lees, W. J.; Whitesides, G. M. *J. Org. Chem.* **1993**, *58*, 642−647 and references therein.
(10) Kajihara, Y.; Kodama, H.; Endo, T.; Hashimoto, H. *Carbohydr. Res.* **1998**, *306*, 361−378.

Scheme 1

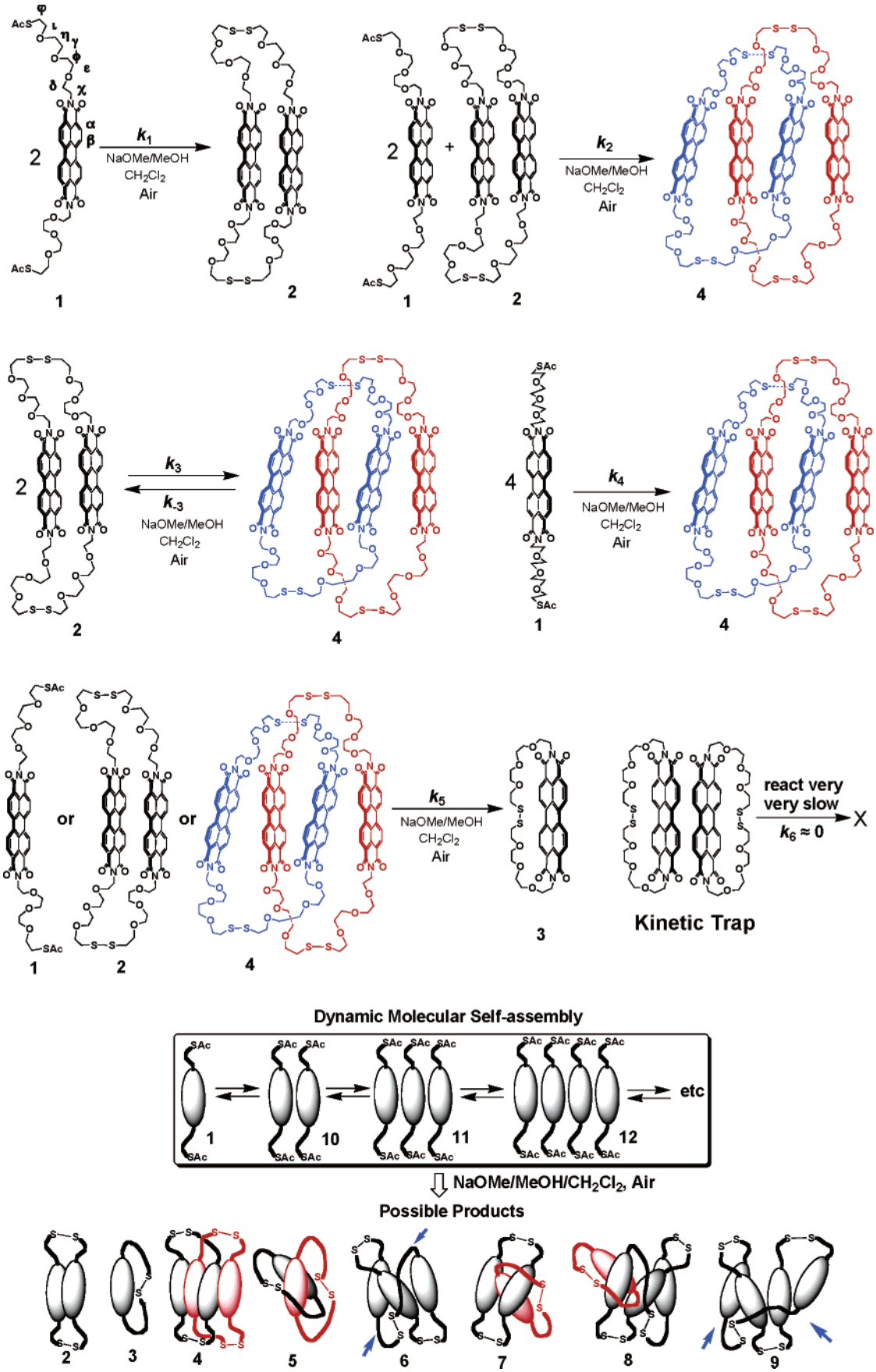

and CH_2Cl_2 solvents (Scheme 1).[7,11] Accordingly, a series of CH_2Cl_2 solutions of **1** under air at concentrations immediately above or below the C_c, namely 2.58 mM, 0.58 mM, and 0.1 mM, respectively, was investigated. Deacetylation of **1** (−Ac)

with several drops of 2 M NaOMe/MeOH formed reactive intermediate counterparts of **1** in solution (solution color changes from red to blue), which subsequently yielded various cyclic compounds linked by disulfide bonds upon air oxidation (TLC R_f: 0.24 to 0.42, CH_2Cl_2/MeOH: 20/1).[12] Of particular interest was that only two major products were obtained, dimer-based monocyclic disulfide **2** and its catenane **4** (Scheme 1) after Amberlite IR-120*(H) neutralization of the reactions. HPLC analysis for the reaction of 0.58 mM reactant **1** yielded ~39% for **2** and ~36% for **4**, a total isolated yield of ~75%, and other unidentified products including trace amounts of polymers.

In principle, many other cyclic structures such as **5**, **6**, **7**, **8**, **9**, etc. could have formed from reactant **1** or its assemblies **10**, **11**, **12**, and so on, but in practice, dynamic self-assembly chooses to amplify only two products, **2** and **4**, at the expense of the others. Thermodynamically, all these cyclic compounds have approximately the same formation enthalpy per monocyclic unit ($C_{40}H_{40}N_2O_{10}S_2$) because they have exactly the same number and the same types of primary bonds. The difference among them comes from secondary $\pi-\pi$ stabilization. Both cyclic dimer **2** and its catenane **4** have favorable π-stacked conformations and should be among the thermodynamically stabilized cyclic compounds with restricted lateral and longitudinal offsets from the energy-minimized perylene stacks.[13] However, the π-stacking contribution to the stabilization energy is small, and cyclic dimer **2** and its catenane **4** have approximately −3 to 5 kcal/mol of extra stabilization enthalpy[14] due to π-stacking and are by no means located in deep potential energy wells. In fact, they were formed through thermodynamically stable organization (an enthalpy effect) directed by DSA, which brought the two thiol groups into proximity for disulfide bond formation (an entropy effect). The monocyclic dimer ring **2** was produced by two disulfide linkages between the nearest stacked building blocks of **1**, and catenane **4** was formed by reactions between the next nearest neighboring thiol groups in the assembly of **1** (these thiol groups yield disulfide bonds that are colored either red or blue in Scheme 1).

In dilute solution (0.1 mM) of **1**, the reaction proceeded quantitatively through face-to-face ordered assemblies of perylene and resulted in the most favorable structures, monocycle **2** and catenane **4**. At a more dilute concentration (0.03 mM), unimolecular self-cyclization occurred and the monocyclic ring **3** was obtained as the third major product. These results revealed that, at or above the critical concentration, the bimolecular reaction product **2** formed before the unimolecular product **3** because of the acceleration effect of DSA. Below the critical concentration, C_c, the unimolecular reaction became competitive, especially under the influence of other directing or templating effects.[15] The presence of methanol in the self-assembly system of **1** is a driving factor toward organization, thus potentially lowering the C_c value.

Unlike dimer ring **2** and the dimer−dimer catenane **4**, other ring compounds are not directed by DSA. In other words, the two specific sulfur atoms required to form a disulfide bond are not brought together by DSA. For example, formation of concatenated rings **5**, **7**, and **8** requires the two adjacent perylene units to form π-stacking with an angle close to 90°. However, our ab initio calculations at the MP2 level suggest that the perylene units prefer a more parallel conformation with a 30° rotation as the minimum energy conformation; other angles are even less favorable. Due to the lack of a self-assembly driving effect, the formation of catenanes with *N* perylene cycles concatenated with a single perylene cyclic monomer should be entropically discouraged. Monocyclic trimer **6** is kinetically disfavored because it requires a sterically inhibited reaction between two thiol groups of the next nearest neighbor atoms (Scheme 1: blue arrows on **6**) that reside on opposite sides of perylene assemblies (sterically prohibited and high transition state energy). Thermodynamically, trimer **6** is also not favored due to disruption of $\pi-\pi$ stacking. Had it formed, it would have been converted to other products. The monocyclic tetramer **9** is not favored by DSA, and only a trace amount was detected by mass spectrometry, because it requires reaction of a sulfur atom with another sulfur atom at the third nearest neighbor position (Scheme 1: blue arrows on **9**), a difficult situation to achieve but still possible.

At an even higher concentration of **1** (2.58 mM), the intermolecular $\pi-\pi$ stacking could drive perylene blocks to form multilayered aggregates, thus leading to a diverse distribution of cyclic structures. In this case at least five main products were found at the beginning of the reaction. However, a dramatic change was observed upon addition of 20% (v/v) methanol to the reaction mixture; only two major products, **2** and **4**, were amplified at the expense of others, and within about 5 min, all other products essentially disappeared. We reason that methanol added to the nonpolar dichloromethane solution could impart hydrogen bonding with TEG side chains (hydrophilic effects) on the side of perylene blocks and, therefore, render the layered aggregates less favorable from an energetic standpoint. This promoted π-stacking of face-to-face linear self-assembled perylene stacks, which consequently amplified formation of the kinetically favorable ring structures as the decisive products, dimer ring **2** and dimer−dimer catenane **4**.

2. Structural Characterization. The ring structures linked by disulfide bonds were characterized using both structural methods (mass spectrometry and NMR) and photophysical measurements (UV−vis). The issue here is how to determine whether the dimer-based macrocyclic disulfide **2** is a monocyclic structure rather than a monomer-based catenane **5** and whether the dimer-based bicyclic disulfide catenane **4** is formed rather than a tetramer-based monocycle **9** or other concatenated structure such as **8**.

The observation of a parent mass peak at $m/z = 1544.5$ (Figure 1A) and fragmentations at 1484.0 ($-SC_2H_4$), 1380.6 ($-S(C_2H_4O)_3$), 1320.3 ($-SS(C_2H_4O)_3C_2H_4$), and 1215.3 ($-(OC_2H_4)_3SS(C_2H_4O)_3$) is consistent with the macrocyclic dimer

(11) (a) Wang, W.; Han, J. J.; Wang, L. Q.; Li, L. S.; Shaw, W. J.; Li, A. D. Q. *Nano Lett*. **2003**, *3*, 455−458. (b) Wang, W.; Wang, L. Q.; Li, A. D. Q. *Chem.−Eur. J.* **2003**, *9*, 4594−4601.

(12) Wallace, T. J.; Schriesheim, A.; Bartok, W. *J. Org. Chem.* **1963**, *28*, 1311−1314.

(13) (a) Rowan, S. J.; Cantrill, S. J.; Cousins, G. R. L.; Sanders, J. K. M.; Stoddart, J. F. *Angew. Chem., Int. Ed.* **2002**, *41*, 898−952. (b) Lam, R. T. S.; Belenguer, A.; Roberts, S. L.; Naumann, C.; Jarrosson, T.; Otto, S.; Sanders, J. K. M. *Science* **2005**, *308*, 667−669.

(14) (a) Wang, W.; Li, L.-S.; Helms, G.; Zhou, H.-H.; Li, A. D. Q. *J. Am. Chem. Soc.* **2003**, *125*, 1120−1121. (b) Wang, W.; Wan, W.; Zhou, H. H.; Niu, S. Q.; Li, A. D. Q. *J. Am. Chem. Soc.* **2003**, *125*, 5248−5249.

(15) (a) Siegel, J. S. *Science* **2004**, *304*, 1256−1258. (b) Andres, P. R.; Shubert, U. *Macromol. Rapid Commun.* **2004**, *25*, 1371−1375. (c) Belfrekh, N.; Dietrich-Buchecker, C.; Sauvage, J. P. *Inorg. Chem.* **2000**, *39*, 5169−5172. (d) Lee, S. J.; Hu, A. G.; Lin, W. B. *J. Am. Chem. Soc.* **2002**, *124*, 12948−12949. (e) Bell, T. W.; Cragg, P. J.; Firestone, A.; Kwok, A. D. I.; Liu, J.; Ludwig, R.; Sodoma, A. *J. Org. Chem*. **1998**, *63*, 2232−2243. (f) Bell, T. W.; Papoulis, A. T. *Angew. Chem., Int. Ed. Engl*. **1992**, *31*, 749−751.

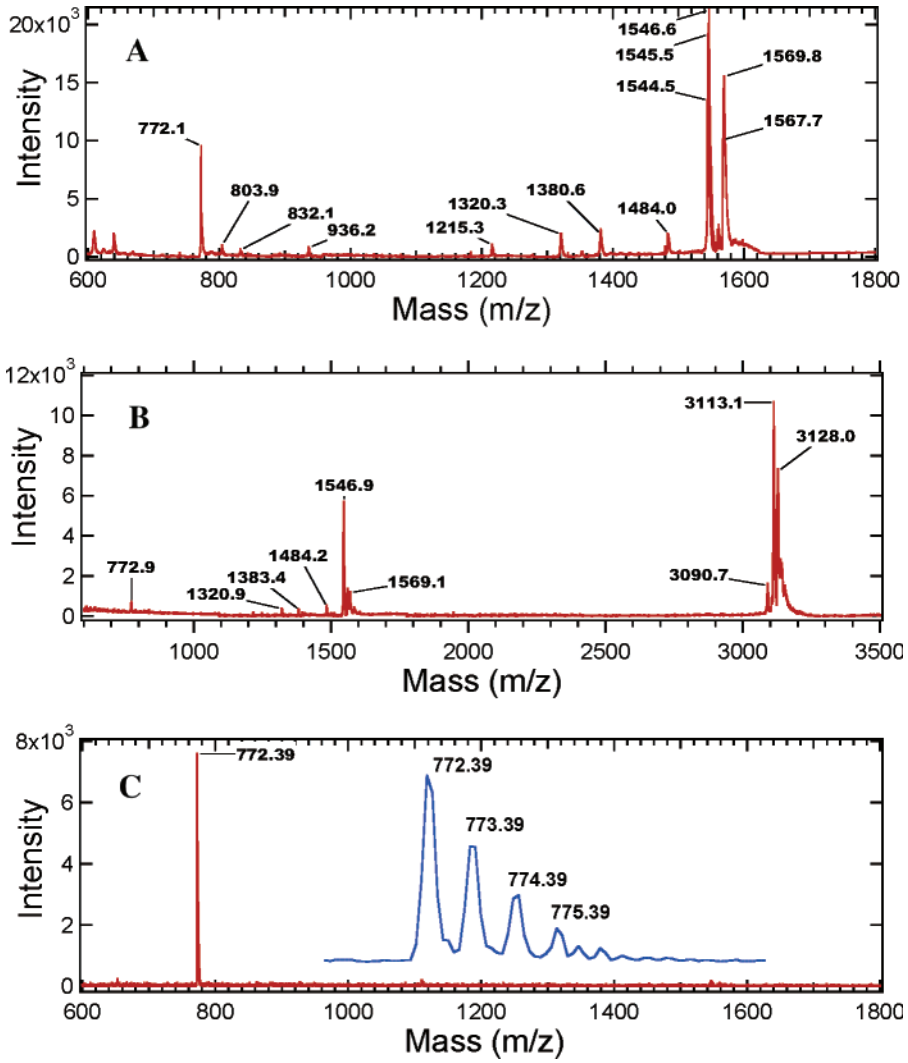

Figure 1. MALDI-TOF mass spectra for (A) dimer−dimer catenane **4**, (B) macrocyclic dimer **2**, and (C) macrocylic monomer **3**. Inset in (C) is an expansion of the peak around 772.39 mass units.

structure **2**. The evidence for concatenated perylene dimer−dimer rings **4** comes from MALDI-TOF measurements (Figure 1B) because there are no ions found between the tetramer parent ion with Na^+ (m/z = 3113.1) and the dimer daughter ions (m/z = 1544.5). A characteristic feature in the mass spectra of catenanes is the total absence of ions between the molecular peak and the peak corresponding to one individual macrocycle.[3b] In other words, residues existing between the molecular peak and the peak corresponding to half (or part) of the ring structure indicate that monocyclization rather than catenation took place. The MALDI PSD (Post Source Decay) data are consistent with the proposed catenane structure (Supporting Information Table 1, 2). Only in dimer−dimer concatenated rings, breaking of any bond will lead to linear and cyclic daughter fragments of half of the parent ion mass. The further fragmentation pattern of the monocyclic daughter ion is identical to that of a macrocyclic perylene dimer **2**, indicating the original parent ion is the dimer−dimer catenane **4**. The monocyclic perylene monomer **3** is also validated by MALDI-TOF mass spectrometry with a strong parent ion at 772.39 having the expected isotope ratios.

Unlike linear oligomer structures, all the observed cyclic structures (**2**, **3**, and **4**) have eight sets of symmetric ethylene chemical resonances in the NMR spectra as shown in Figure 2. The upfield shift and large separation of aromatic protons (Hα and Hβ in Figure 1A and B) indicate a perylene π stack in the ring; this behavior is characteristic of the linear folded perylene dimer and tetramer, in agreement with our early report.[14] Similar to the linear folded perylene dimer and tetramer, the upfield chemical shifts and separation of the bay protons (assigned as proton Hβ) and outer protons (assigned as proton Hα) are dependent on the degree of perylene π-stacking. Consequently, one would expect that the increased upfield shift and separation of the aromatic protons Hα and Hβ should be larger for concatenated dimer−dimer **4** than for monocyclic dimer **2**, which in turn should be larger than those for monocyclic monomer ring **3**. Indeed, this was what we observed, thus confirming that dimer−dimer **4** and monocyclic dimer **2** exist as cyclic *folded* structures. In the concatenated rings **4**, there is little free rotation of one ring with respect to the other because $\pi-\pi$ interactions effectively dock the perylene units on top of each other.

Compared to the dimer rings (**2**, **4**), proton chemical shifts on the TEG chain of **3** (Scheme 1) undergo upfield shifts because they bridge over the perylene segment that imparts an aromatic ring current shielding effect to the TEG chain. For example, the differences of chemical shifts between **3** and **2** in

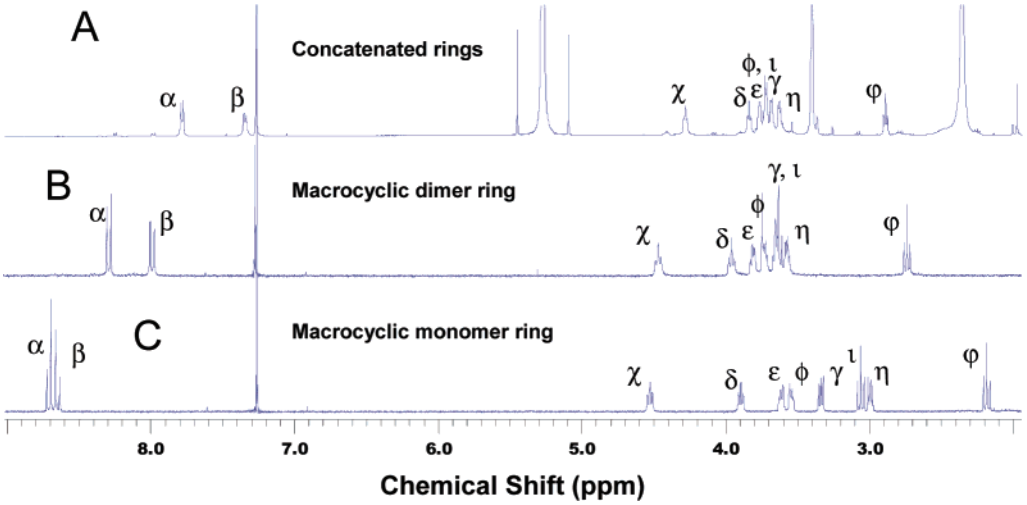

Figure 2. ^{1}H NMR spectra of (A) dimer−dimer catenane **4**, (B) macrocyclic dimer **2**, and (C) macrocyclic monomer **3**. Note the upfield shift of the aromatic protons in catenane **4** and macrocyclic dimer **2** is due to perylene forming stacks and spreading of the aliphatic protons on the TEG chain in the monocyclic monomer **3**.

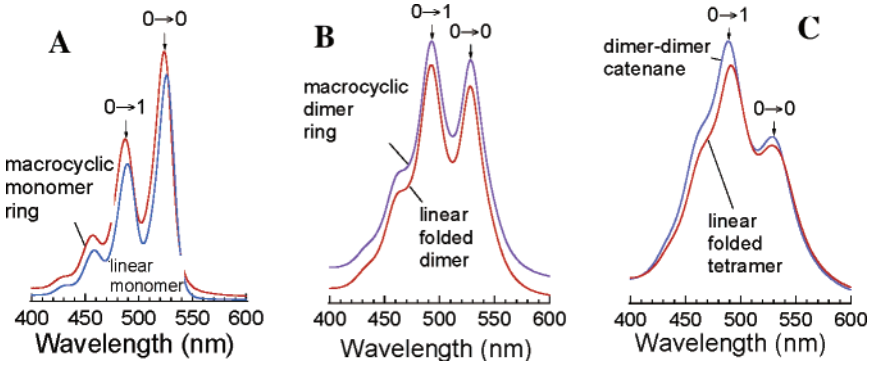

Figure 3. Comparison of UV−visible absorption spectra in CH_2Cl_2 between (A) macrocyclic monomer **3** and linear monomer **1**, (B) macrocyclic dimer ring **2** and linear folded dimer, and (C) dimer−dimer catenane **4** and linear folded tetramer. The optical absorption spectra of folded linear compounds are from ref 15a.

ppm are $\Delta\delta_\epsilon$ ~0.23, $\Delta\delta_\phi$ ~0.23, $\Delta\delta_\gamma$ ~0.36, $\Delta\delta_\eta$ ~0.63, $\Delta\delta_\iota$ ~0.65, and $\Delta\delta_\varphi$ ~0.63 (Figure 2). Additionally, median NOE coupling strengths were observed in monocycle **3** between the protons adjacent to disulfide linkages and the perylene aromatic protons in the 1D GOESY experiment, indicating the "basket" structure of **3**. However, no NOE exists between the protons adjacent to disulfide bonds and those on aromatic rings in the dimer-based cycles (**2**, **4**) because the perylene stack forces the flexible chains far away from the compact aromatic cores.

The above NMR analysis validates that **3** has a monocyclic ring structure and is a monocyclic monomer. For compound **2**, eight sets of symmetric ethylene chemical resonances in the NMR spectrum corroborate that it must be a ring structure because linear structures will yield more than eight sets of aliphatic protons (Figure 2). This is in contrast to compound **3** that does have an NOE; no NOE is observed between aromatic protons and ethylene units in compound **2**. As a result, the structure cannot be concatenated rings as shown in compound **5**. Thus, compound **2** must be a monocyclic dimer. Similarly, the observation of eight sets of symmetric ethylene chemical resonances in the NMR spectrum of **4** indicates that it must be a ring-structured compound. One such compound containing four perylene units has asymmetric concatenated rings; this is compound **8**. Compound **8** has more than eight sets of protons because the two rings are not equivalent, and therefore NMR has ruled out the possibility of asymmetric rings, or **8** being the major product. The only other possibility is that the major product could be the monocyclic tetramer or compound **9**. If the perylene units had no interactions (i.e., no π-stacking) in the monocyclic tetramer **9**, there would be 8 sets of ethylene proton resonances, but the aromatic protons would not shift upfield and the separation between bay protons and outer protons would not occur. In the case of π-stacking, as indicated by the upfield shift and separation of the aromatic protons, there will be more than 8 sets of protons for the monocyclic tetramer **9**. Therefore, the simultaneous observation of the upfield shift and the separation of outer-bay protons and the 8 sets of symmetric ethylene protons (Figure 2) has ruled out the possibility of compound **9** being the major product. This leads to the conclusion that compound **4** must have a concatenated dimer−dimer ring structure.

Perylene folded in a stacking motif shows a remarkable intensity reversal between the vibronic 0 → 0 band and 0 → 1 band in the electronic absorption of the π to π^* transition. Accordingly, the monocyclic perylene monomer **3** should resemble the free perylene derivative such as **1** as shown in Figure 3A. Similarly to the linear folded dimer, the optical absorption spectrum of **2** shows a reversal of vibronic 0 → 0 and 0 → 1 band intensity (Figure 3B), confirming a ring with one perylene unit docking on another. This docking behavior is also observed in molecular rotors where one molecular unit preferentially docks to another unit on the ring due to attractive

interactions.[16] Optical absorption of catenane **4** is almost identical to the linear folded tetramer, proving that the four perylene units are π-stacked (Figure 3C). The results of optical absorption studies of catenane **4** support the NMR assignment of a concatenated dimer−dimer ring structure.

3. Kinetics and Mechanistic Analyses. According to an equal-*K* model,[11] the concentration of the self-assembled dimer **10** should be much larger than the self-assembled trimer **11**, which is much larger than the self-assembled tetramer **12**, i.e., [**10**] ≫ [**11**] ≫ [**12**] and so on for higher n-mers. This can readily explain the formation of cyclic dimer **2** (k_1) because the dominating self-assembled dimer **10** serves as its precursor. However, this model does not explain why catenane **4** should be the second major product. To shed light on the formation of the catenane, we systematically investigated all three possible routes to catenane **4** as shown in Scheme 1. Specifically, catenane **4** can come from the reaction of linear monomer **1** and cyclic dimer **2** (k_2), or two cyclic dimers **2** (k_3), or four linear monomers **1** (k_4). The whole DSA system can be described with eqs 1−3.

$$-\frac{d[\mathbf{1}]}{dt} = 2k_1[\mathbf{1}]^2 + 2k_2[\mathbf{1}]^2[\mathbf{2}] + 4k_4[\mathbf{1}]^4 \quad (1)$$

$$-\frac{d[\mathbf{2}]}{dt} = k_2[\mathbf{1}]^2[\mathbf{2}] - k_1[\mathbf{1}]^2 + 2k_3[\mathbf{2}]^2 - 2k_{-3}[\mathbf{4}] \quad (2)$$

$$\frac{d[\mathbf{4}]}{dt} = k_2[\mathbf{1}]^2[\mathbf{2}] + k_3[\mathbf{2}]^2 - k_{-3}[\mathbf{4}] + k_4[\mathbf{1}]^4 \quad (3)$$

To solve the above coupled equations, we divide the system into an initial period and a steady-state period. In the initial period, $t < \tau$ ($\tau = 25$ min for 0.58 mM of **1**), the major product is **2** and no appreciable catenane **4** is formed (Figure 4A), the system of equations is simplified into a single second-order reaction as described by eq 4. In fact, the formation of **2** follows second-order reaction kinetics remarkably well, yielding a rate constant of $k_1 = 0.213 \pm 0.003$ mM^{-1} min^{-1} (Figure 4B), while $[\mathbf{2}]k_2 \approx k_3 \approx k_4 \approx k_5 \approx 0.0$.

$$-\frac{1}{2}\frac{d[\mathbf{1}]}{dt} = \frac{d[\mathbf{2}]}{dt} = k_1[\mathbf{1}]^2 \quad (4)$$

In the steady-state period, $t > \tau$, the concentration of **2** becomes constant, i.e., d[**2**]/d$t \approx 0$. The major new product is catenane **4**. A trace amount of monocyclic tetramer **9**, having a slightly lower elution time than that of the dimer−dimer catenane, was captured with HPLC (Figure 2A) and verified by MALDI (Supporting Information Figure 4). If the catenane **4** was formed predominantly from four monomers (i.e., $k_4 \gg k_2$ and k_3), one can see that the concentration, [**4**], of catenane **4** should increase linearly as a function of time initially when [**1**] is approximately constant; this is not observed in Figure 4C. The result here agrees with the equal-*K* model where the contribution to catenane **4** from self-assembled **12** is negligible ($k_4 \approx 0$).

To identify which pathway leads to major catenane **4** formation, we have examined the following specific reactions. First, the cyclic dimer **2** was treated with the exact same reagents used in reactions of monomer **1**. Within the time period of **1** where the catenane **4** is produced, the cyclic dimer **2** hardly forms any catenane **4**, indicating that the rate constant k_3 is very small ($k_3 \rightarrow 0$) but not zero. This eliminates from consideration that the major pathway to catenane **4** is through dimer−dimer interaction and subsequent exchange of disulfide bonds. Similarly, we have verified that the reverse reaction from catenane **4** to cyclic dimer **2** is also very slow ($k_{-3} \rightarrow 0$) but not zero. Thus, the disulfide exchange reactions in this system appear to be kinetically rather slow. The only pathway left to catenane **4** is if the cyclic dimer interacts with two linear monomers **1**. As noted earlier, monomer **1** does not yield an appreciable amount of catenane **4** until the cyclic dimer **2** has reached a steady state. However, upon addition of one-third of an equivalent of cyclic dimer **2** to monomer **1**, catenane **4** formation was immediately observed with TLC. This supports the contention that the major pathway to catenane **4** is through interaction of a cyclic dimer with two monomers **1**.

In the steady-state approximation (SSA) period ($t > \tau$), the above equations (1−3) are reduced to eqs 5 and 6. The major pathway to catenane **4** is a pseudo second-order reaction with respect to monomer **1** with the concentration of **2** being constant, $[\mathbf{2}]_{SSA} = 0.22$ mM. Fitting eq 5 with the experimental data in Figure 2B, we obtain an apparent rate constant of $k_1 + k_2[\mathbf{2}]_{SSA} = 1.38 \pm 0.02$ mM^{-1} min^{-1}, which yields a third-order rate constant $k_2 = 5.32 \pm 0.09$ mM^{-2} min^{-1}. Solving eqs 5 and 6 also reveals that the concentration increase in catenane **4** is directly proportional to the concentration decrease of **1** at $t > \tau$ (see eq 7); this kinetic model agrees with experimental results remarkably well as shown in Figure 4C.

$$-\frac{1}{2}\frac{d[\mathbf{1}]}{dt} = (k_1 + k_2[\mathbf{2}]_{SSA})[\mathbf{1}]^2 \quad (5)$$

$$\frac{d[\mathbf{4}]}{dt} = k_2[\mathbf{2}]_{SSA}[\mathbf{1}]^2 \quad (6)$$

$$d[\mathbf{4}] = -\frac{k_2[\mathbf{2}]_{SSA}}{2(k_1 + k_2[\mathbf{2}]_{SSA})} d[\mathbf{1}] \quad (7)$$

To validate that the pathway to catenane **4** is mainly from cyclic dimer **2** and monomer **1**, the kinetics of the cyclization reaction between **1** and **2** was measured. The reaction proceeded directly to the formation of catenane **4** as a pseudo second-order reaction during the initial stage of the reaction. Because of the presence of the SSA intermediate (monocyclic dimer **2**) the pre-steady-state period was not observed. When the reaction was started with an initial concentration of $[\mathbf{2}]_{SSA} = 0.45$ mM, an apparent rate constant observed for consumption of monomer **1** was $k_{obsd} = k_1 + k_2[\mathbf{2}]_{SSA} = 2.87$ mM^{-1} min^{-1} from the data in the first 6 min after mixing of cyclic dimer **2** and monomer **1**. Using the value of $k_1 = 0.21$ mM^{-1} min^{-1}, the reaction rate constant k_2 is determined to be 5.91 mM^{-2} min^{-1}, which agrees remarkably well with the steady-state approximation value of $k_2 = 5.32$ mM^{-2} min^{-1}.

To form concatenated rings, the intermediate species must have one monomer associated with the cyclic dimer. However, such an intermediate is too elusive to be captured in a stable configuration. The kinetic data support the formation of such an unstable intermediate complex of **1**·**2**, which subsequently

(16) (a) Leigh, D. A.; Wong, J. K. Y.; Dehez, F.; Zerbetto, F. *Nature* **2003**, 174−179. (b) Balzani, V.; Credi, A.; Raymo, F. M.; Stoddart, J. F. *Angew. Chem., Int. Ed.* **2000**, *39*, 3348−3391.

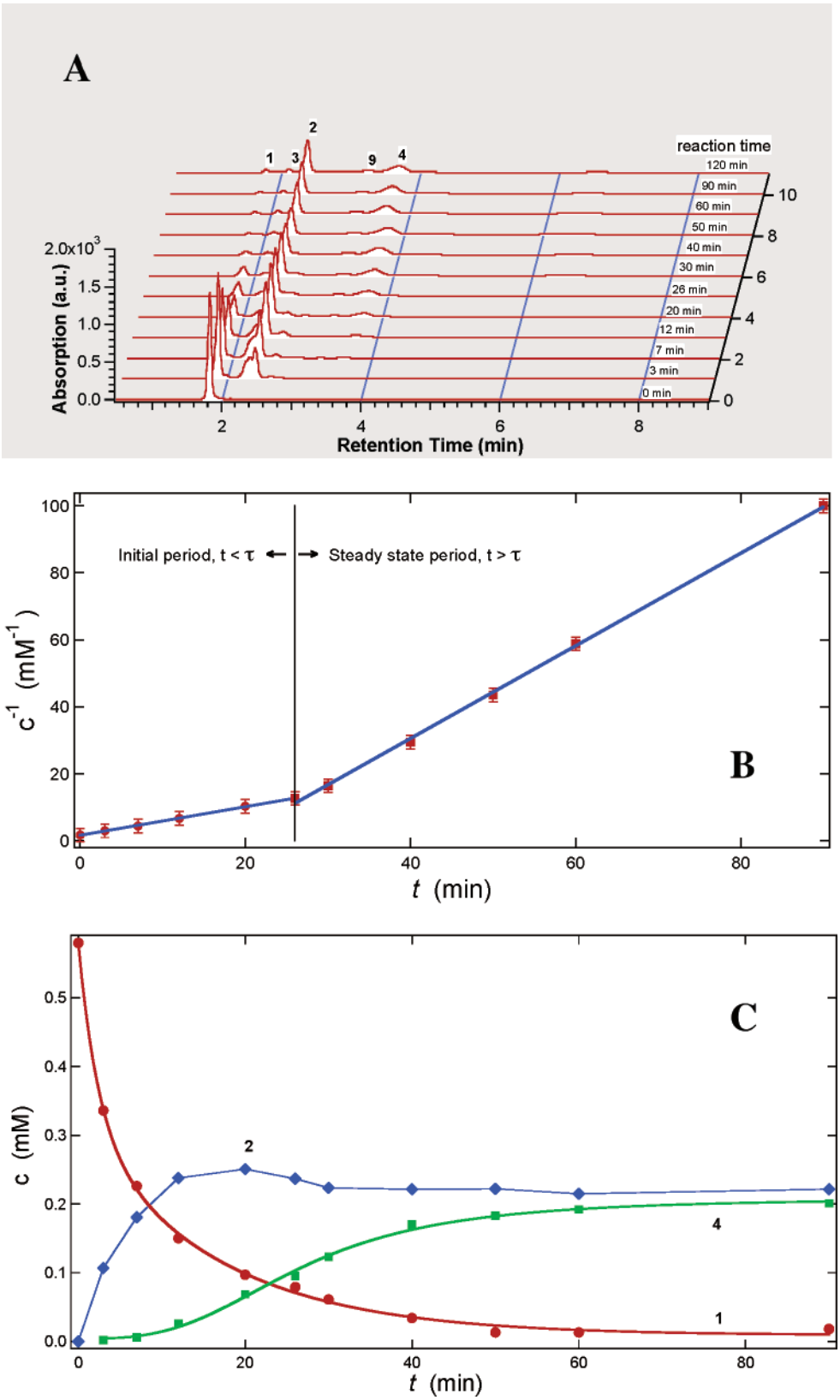

Figure 4. (A) HPLC monitoring of the disulfide ring closure of **1** at 0.58 mM at various reaction times. (B) After the first 25 min, cyclization forms mainly a cyclic dimer via a second-order reaction, and the reaction then enters a steady state to form the concatenated dimer−dimer ring and proceeds as a pseudo second-order reaction with respect to monomer **1**. (C) Plots of the monomer **1**, cyclic dimer **2**, and dimer−dimer catenane **4** concentrations as functions of reaction time. Note the dimer concentration reaches a steady state soon after the reaction.

reacts with another monomer **1** as shown in eq 8. The rate-determining step (k_{2b}) involves closure of the concatenated ring; in this situation, the rate of catenane **4** formation will be first-order with respect to the monocyclic dimer **2** and second-order with respect to the linear monomer **1**, in excellent agreement with experimental observations.

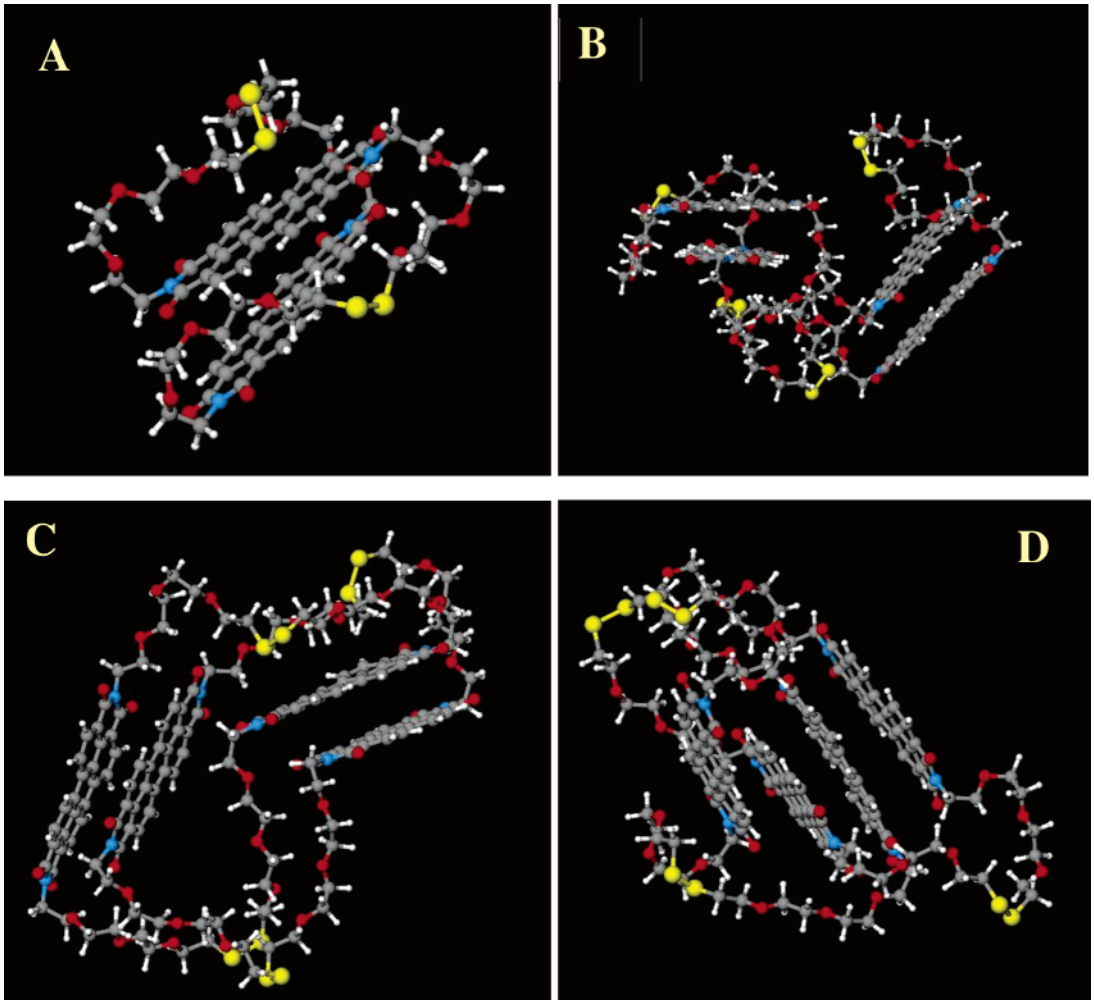

Figure 5. (A) A single perylene dimer ring showing the two stacked perylene units. (B) In the concatenated perylene dimer rings, two perylene units, which form stacks, are both part of the same dimer ring (cis configuration). (C) The perylene units are stacked in the trans configuration in which the two stacked perylene units are each on separate dimer rings that are concatenated. (D) Two concatenated perylene dimer rings. All four perylene units are stacked on top of each other.

To simplify the complex dynamic self-assembly system, the pathways to major products are summarized in the reactions below. However, other pathways and interconversion do exist, and they contribute minor amounts of the products under the experimental conditions used.

$$\mathbf{1} + \mathbf{1} \underset{k_{-1a}}{\overset{k_{1a}}{\rightleftharpoons}} \mathbf{1{\cdot}1} \xrightarrow{k_{1b}} \mathbf{2}$$

$$\mathbf{1} + \mathbf{2} \underset{k_{-2a}}{\overset{k_{2a}}{\rightleftharpoons}} \mathbf{1{\cdot}2} \xrightarrow[\mathbf{1}]{k_{2b}} \mathbf{4}$$

$$\frac{\mathrm{d}[\mathbf{4}]}{\mathrm{d}t} = k_{2b}[\mathbf{2{\cdot}1}][\mathbf{1}] = \frac{k_{2a}k_{2b}}{k_{-2a}}[\mathbf{1}]^2[\mathbf{2}] = k_2[\mathbf{1}]^2[\mathbf{2}] \qquad (8)$$

Interestingly, the monocyclic monomer **3** is not thermodynamically more stable than other cyclic products such as catenane **4** and cyclic dimer **2** based upon formation enthalpy analyses (*vide supra*); nonetheless it accumulates in the system. This is because it reacts very slowly due to the fact that self-assembly neither juxtaposes S−S bonds in a way that promotes disulfide exchange nor reacts favorably with thiol ester groups via a deacetylation reaction (Scheme 1; k_6). Since **3** has a basket shape, cofacial assembly of **3** can only occur via the bottom−bottom approach to form self-assembled dimers of **3**. Such interactions, however, effectively separate the two disulfide bonds on opposite sides of the reaction sphere, and therefore disulfide exchange nearly ceases. In other words, compound **3** is a *kinetic trap* for disulfide exchange or other ring formation reactions, although catenane **4** and cyclic dimer **2** can be stored at −20 °C in organic solvents for months; at room temperature they remain in dynamic equilibrium under the original basic reaction conditions and exchange very slowly (k_3 and k_{-3}) and yet *reversibly* among themselves. Conversion of catenane **4** and cyclic dimer **2** to **3**, a compound formed only as a trace amount byproduct when self-assembly governs the system, is mostly *irreversible* because of the kinetic trap. In fact, monocycle **3** is disfavored both kinetically and thermodynamically in the above reactions except when $C \ll C_c$ (e.g., [**1**] = 0.03 mM). Compared to the dimer-based cycles, **3** is thermodynamically less stable than the cyclic dimer by ∼3 kcal/mol[14a] due to the lack of extensive π-stacking. Experimental kinetic data have shown that its formation cannot compete with the formation of the cyclic dimer when DSA promotes cyclization reactions. In the initial basic solution, both catenane **4** and cyclic dimer **2** eventually convert to **3** when sufficient time (days) is allowed. The reason for accumulation of **3** is that disulfide bonds are "caged" for disulfide exchange reactions in the unique monocyclic structure;

this does not imply that disulfide bonds are thermodynamically stable. Such a caging phenomenon results in a kinetic trap, rather than the well-known thermodynamic trap, for monocyclic monomer **3**. Because of the kinetic trap, pure **3**, which was originally synthesized by a different pathway (Supporting Information), is kinetically "stable," while pure **2** or **4** slowly interconvert and are finally trapped as **3** under the original deacetylation conditions.

4. Molecular Dynamics Modeling. To gain further insights into the dynamic behavior of the cyclic dimer **2** and its catenane **4**, we have carried out molecular dynamics simulations. Simulations of both the monocyclic dimer **2** and its concatenated dimer−dimer **4** rings were performed in dichloromethane. The simulations were done using the NWChem molecular dynamics software module.[17] The setup and visualization of the simulations were performed using a prerelease version of the Extensible Computational Chemistry Environment (Ecce) version 4.0[18] that is being developed to provide a user interface for creating and executing molecular dynamics simulations using NWChem. The solvent parameters are based on Fox and Kollman's model for dichloromethane.[19] No parameters for the perylene dimer exist in the literature, so a model for this system was developed based on parameters available in the Amber force field.[20] The partial charges were assigned using a standard methodology described in the literature.[19] Initial configurations of both the single ring and concatenated rings were created using the molecular builder module in Ecce and then solvated with dichloromethane using the NWChem prepare module. Long simulations at constant pressure and temperature (1 atm and 25 °C) were done to equilibrate the system followed by simulations of 150 ps to observe the configurational behavior of the ring systems.

A variety of simulations of the monocyclic dimer ring **2** were done; the main difference between the simulations was the initial configuration of the perylene dimer ring. Simulations in which the initial configuration of the ring was chosen so that the perylene molecules were not placed on top of each other in a relatively relaxed configuration did not result in stacking of the perylenes over the simulation time. Instead, one of the chains holding the two perylene units together tended to slip between the plates and keep them apart. This behavior persisted over the course of the simulation. Additional simulations of 150 ps or so did not result in stacking, suggesting that the time scale for stacking is much longer than the accessible simulation time. However, if the initial configuration was chosen so that the perylene units are carefully stacked in a relaxed configuration at the start of the simulation, then the perylene units remain stacked. A configuration from one of these simulations is shown in Figure 5A. The results are consistent with a conversion between the stacked and unstacked configurations seen in the experiment, but the time scales accessible in the simulations are too short to observe the conversion directly.

Simulations of the concatenated dimer−dimer catenane **4** showed contrasting behaviors. The concatenated rings contain a total of four perylene units. Two configurations were found in which the perylene units stack in two pairs, and another configuration was found in which all four perylenes form a single stack. The two configurations in which the perylene units pair up consist of a "cis" configuration, where the perylene units on the same ring are paired, and a "trans" configuration where perylene units on opposite rings are paired. Snapshots of the cis and trans configurations are shown in Figure 5B and 5C. A snapshot of the configuration containing four stacked perylene units is shown in Figure 5D. Over the course of the simulations, all three configurations appear to be stable and no sign of interconversion between the structures was observed. Again, this suggests that the time scale for interconversion, if it occurs, is longer than the time scales accessible by these simulations.

Conclusions

With a deeper understanding of the molecular self-assembly process, we begin to appreciate that formation of strong covalent bonds is intrinsically linked to weak secondary interactions, such as ion pairing or dipolar interaction. While molecular self-assembly employs weak interactions to form various nanostructures, their potential functions to direct or template specific reaction pathways have not been widely exploited. We demonstrated here that novel reactions could be promoted by molecular self-assembly and these reactions would be difficult to carry out otherwise. Dynamic molecular assembly effectively directs particular ring closure reactions; consequently, cyclic dimer **2** becomes the immediate major product. This cyclic dimer then guides the formation of a dimer−dimer catenane **4**, which becomes the second major product. This understanding sets the stage for exploring the use of DSA to direct specific reaction pathways to novel chemical structures.

Acknowledgment. The authors acknowledge the support of the National Institute of General Medical Sciences (Grant GM065306), the Arnold and Mabel Beckman Foundation, and the U.S. Department of Energy (DOE), Office of Basic Energy Sciences, Division of Materials Science and Engineering Physics. A.D.Q.L. is a Beckman Young Investigator (BYI). We thank Ms. Maggie Tam and Dr. William Siemes for assistance in mass spectrometry and Dr. Greg Helms for NMR measurement.

Supporting Information Available: Procedures for the preparation of compound **1**, monocyclic monomer ring **3**, experimental details about characterization of monocyclic dimer **2** and its concatenated tetramer **4** by mass spectrometry, and determination of the reaction yields of compound **2** and **4** by HPLC. This material is available free of charge via the Internet at http://pubs.acs.org.

JA061826P

(17) Kendall, R. A.; Apra, E.; Bernholdt, D. E.; Bylaska, E. J.; Dupuis, M.; Fann, G. I.; Harrison, R. J.; Ju, J.; Nichols, J. A.; Nieplocha, J.; Straatsma, T. P.; Windus, T. L.; Wong, A. T. *Comput. Phys. Commun*. **2000**, *128*, 260−283.

(18) Black, G. D.; Schuchardt, K. L.; Gracio, D. K.; Palmer, B.; The Extensible Computational Chemistry Environment: A Problem Solving Environment for High Performance Theoretical Chemistry; In *Computational Science − ICCS 2003, International Conference Saint Petersburg Russian Federation, Melbourne, Australia, Proceedings 2660*; Sloot, P. M. A., Abramson, D., Bogdanov, A. V., Dongarra, J., Eds.; Springer-Verlag, Berlin, Germany, 2003; Vol. 81, pp 122−131. See also http://ecce.pnl.gov.

(19) Fox, T.; Kollman, P. A. *J. Phys. Chem. B* **1998**, *102*, 8070−8079.

(20) Cornell, W. D.; Cieplak, P.; Bayly, C. I.; Gould, I. R.; Merz, K. M.; Ferguson, D. M.; Spellmeyer, D. C.; Fox, T.; Caldwell, J. W.; Kollman, P. A. *J. Am. Chem. Soc*. **1995**, *117*, 5179−5197.